STUDY OF MECHANICAL PROPERTIES, MICROSTRUCTURE AND RESIDUAL STRESS BY X-RAY DIFFRACTION IN WELDED JOINTS OF DUPLEX STEEL UNS S 31803 BY COATED ELECTRODE

M. C. L. Souza[a], W. D. Badaró[a] V. I. Monine[b] C.A.M. Ferreira[a], and N. C. O. Tapanes[a]

[a] State University of Rio de Janeiro Av. Manuel Caldeira de Alvarenga, 1203, Rio de Janeiro - RJ, 23070-200, Brasil mauro.souza@uerj.br

[b] Polytechnic Institute of the State of Rio de Janeiro. R. Hormindo Silva, 25 - Lagoinha, Nova Friburgo - RJ, 28625-570, Brasil

Received: Aug 20, 2022
Revised: Aug 23, 2022
Accepted: Aug 27, 2022

ABSTRACT

Duplex stainless steels are widely used in the chemical, nuclear and oil and gas industries. They have an austenitic-ferritic microstructure, in equal parts. In this work, the impacts on the mechanical properties, on the metallographic behavior and the analysis of the residual stresses caused after the welding process by coated electrode were analyzed. In these analyses, a specimen produced from a 10 mm thick duplex sheet was welded, and tensile tests, micrography and residual stress analysis by x-ray diffraction were carried out. The tensile test results showed values higher than those required by the material's manufacturing standard. The specimens broke in the base metal during the tests, indicating that the welding parameters were properly specified and applied to the specimen. The metallographic analysis showed an increase in the ferritic phase in the weld region, which makes this region susceptible to pitting corrosion in environments containing chlorides. Residual stress analysis showed tensile stresses in the weld bead, in the longitudinal and transverse directions, and in the HAZ and in the root compressive stresses in the transverse direction and tensile stresses in the longitudinal direction. These stresses must be considered in the design of equipment and structures manufactured from this steel and when using coated electrode welding, to avoid premature failure, especially fatigue failure.

Keywords: Tensile tests; X-ray diffraction, residual stresses; micrography

INTRODUCTION

Duplex stainless steels are widely used in chemical, nuclear and oil and gas industries due to their excellent corrosion resistance, high mechanical strength and good toughness. In these sectors, the use of duplex steels almost always involves welding processes accompanied by stresses in the weld regions. Duplex, comes from Latin and means double, and steels that have a microstructure formed by two distinct phases are called such: ferrite and austenite, which when they are in approximately equal amounts, obtained by solubilization treatment, present better properties (Alvarez, 2008; Evangelista, 2004). For the duplex stainless steel sheets in this work, ASTM A240 (2014) is applicable (ASM HANDBOOK, 1990). This standard requires that the annealing heat treatments applied to duplex stainless steel grade UNS S31803 occur in the range between 1020°C and 1100°C (Karlson, 1991; Loureiro, 2010; Gunn, 2003).

In the manufacturing processes, or forming of metallic parts, stresses are introduced. In manufacturing, the objective is a process that introduces the least possible tensions to the final product, however, a process that does not introduce any tension to the final product is impossible (Chiaverini, 2002).

Stresses that arise during the manufacturing process are called residual stresses. These can be introduced during the use of manufacturing processes such as mechanical forming, rolling, heat treating and welding operations (Ribeiro, 2021).

The presence of residual stresses in materials and components can have an important influence on their behavior, as they can greatly alter the fatigue life resistance, the ability of these materials to withstand loading and fracture resistance (Sieurin, 2006) since these tensions are superimposed on the applied tension, increasing or reducing the effective tension according to its nature (tractive or compressive). Normally, the processes that result in surface compression are beneficial and increase fracture resistance, but can cause warping, while those that produce tensile stresses that generally cause the appearance of cracks that can lead to premature failure (Monine, 1994).

In manufacturing processes of parts and components by welding, a temperature gradient occurs around the welded region. This introduces residual stress due to heterogeneous heating and cooling of the parts. In the heat-affected zone (HTA),

next to the molten zone, grain growth occurs due to the increase in temperature and, therefore, the crystalline structure will be modified. Due to these factors, the material can fracture in this region (Chang, 2004).

There are several methods available to measure and evaluate these voltages. They can be destructive, such as those using strain gauges, or non-destructive, such as x-ray diffraction, neutron diffraction and ultrasound.

MATERIAL AND METHODS

Material

In this paper, an ASTM A240 UNS S31803 duplex sheet was used, measuring 235 mm wide by 640 mm long and 10 mm thick and with chemical composition according to the raw material certificate in Table 1. Four 100 mm pieces were cut from this sheet. in width by 160 mm in length, using a cutting disc suitable for cutting stainless steel, to produce two specimens. Figure 1 details the dimensions of the specimen after the welding process.

Table 1. Maximum Chemical Composition of Base Metal Grade 316L - ACESITA Certificate.

C	Mn	Si	P	S	Cr	Ni	Mo	N
0.03	1.95	0.098	0.03	0.015	23.0	6.4	3.4	0.14

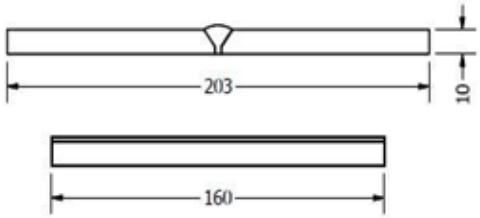

Figure 1 – Dimensions of the Specimen used in the welding.

As a consumable, a coated electrode was used, according to AWS A5.4 specification, classification ER220917, with a diameter of 3.25 mm, with the BÖHLER FOX CN 22/9 N electrode, welded in the 1G position (Marques, 2007).

Methods

The V-bevel was used for welding. The preparation of the bevels was carried out by cutting and grinding followed by a visual test. The bevel angle = 37.5o

The plates were assembled with a spacing between the chamfers of 3 mm and with the aid of small transverse plates at the ends to help finish the weld bead (Folkhard, 1997).

Welding was performed in the flat position (1G), in multiple passes, according to parameters described in table 2. Welding parameters used as suggested by the electrode manufacturer.

Table 2. Welding Parameters (MARQUES, 2007)

Filler Metal	Classif.	ER2209-17
	Ø (mm)	3.25
Current	Type	CC+
	Value (A)	70 - 140
Voltage	(V)	20-25
Temperature (°C)	Pré	≥15
	Interpass	≤85
Thermal input (kj/mm)		0.65-0.93

Tensile Test

Three specimens were made in the Physics laboratory of COPPE-UFRJ, taken transversally to the weld bead. Figure 2 shows the specimen.

Figure 2 - Specimen as manufactured.

The tensile tests were performed at room temperature (25°C), in standardized bodies according to ASTM A 370, shown in figure 3 and Table 3 (Chen, et al., 2001). The profiles of the specimens using a NIKON PROFILE PROJECTOR MODEL 6C projector (Chang et al. 2004).

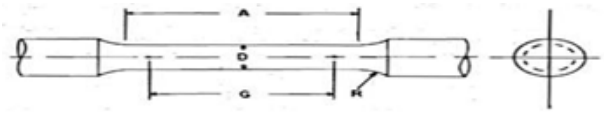

Figure 3 - Tensile test specimen (ASTM A 370)

Table 3. Dimensions of the specimen

	Standard specimen
Nominal diameter, in	0.25
G- Useful length, in	1.0 ± 0.005
D- Diameter, in	0.25 ± 0.005
R- Fillet radius, in	3/16
A- Reduced section length, in	1 1/4

The specimen profiles using a NIKON PROFILE PROJECTOR MODEL 6C projector. These profiles are shown in table 4. After collecting the profiles, tensile tests were performed using a universal testing machine EMIC line DL 100 kN. Figure 4 shows the specimen during testing.

Table 4. Specimens Test

Specimens	SP1	SP2	SP3
Length (mm)	38,27	37,89	38,49
Diameter (mm)	6,05	6,21	6,02

Figure 4 - Specimen during the test.

From the loading curves, the yield point (σy) and the resistance limit (σr) were raised. The percentage of area reduction (RA%) and the percentage elongation (A%) were obtained from dimensional measurements performed on the tested specimens (Pinto, 2009).

Micrograph

Microstructural characterizations were performed at 50X magnification. The microstructures of the samples were analyzed after chemical attack Nital 2% and microscopic observation. The microstructural identification and its correlations in the cut region.

The samples for metallographic analysis were prepared and followed the following preparation steps: Cutting, sanding with sandpaper with granulometry from 100 to 2500 mesh, followed by polishing with diamond paste with granulometry of 3μm and 1μm, after the chemical attack using glyceregia composed of 5ml of glycerin, 15ml of hydrochloric acid (HCl), 10ml of acetic acid and 10ml of nitric acid (HNO3), where the samples were submerged for 30 seconds in the reagent and ending with microscopic observation in the metallographic analysis laboratory of COPPE-UFRJ, in the LEICA Microscope, model DMRM.

Residual Stress Analysis

Cleaning the weld region of the plates introduces residual stresses in the surface layer that add to the residual stresses generated by the welding process. Therefore, an electrolytic polishing of an area of X-ray diffraction stress measurements was performed equal to 10x10 mm2 with a removed layer thickness equal to 0.15 ÷ 0.2 mm.

Residual stress measurements were performed using a mini diffractometer developed in the physics laboratory of UERJ.

According to the methodology of stress measurements by "square sine of psi" method, it is necessary to process the diffraction line profile to determine the value of diffraction angle θ and build a graph θ = f(sen2ψ).

As duplex steel is a composite material that contains approximately equal amounts of ferritic and austenitic phases and x-ray diffraction is a selective phenomenon, therefore, each phase diffracts separately. Therefore, voltage measurements were carried out in both the ferritic and austenitic phases. For residual stress measurements, the reflections (hkl) of the crystalline planes (211) and (220) were used for ferrite and austenite respectively. The values of the diffraction angles corresponding to these phases and reflections using a Cr anode x-ray tube are θ211 = 77.010 of ferrite and θ220 = 63.580 of austenite

In this work, the diffraction angle θ is determined by processing the diffraction line profile obtained with a position-sensitive detector. The formula for converting the detector channel into diffraction angle grain depends on the technical characteristics of the detector and the distance between the detector and the analyzed sample. For the mini diffractometer used, the conversion formula can be written as (MONINE, et al, 1994):

$$\theta = k*N\ (\ 0\ /canal\ )$$

where k is the conversion coefficient of the channel number in degree of diffraction angle. With this coefficient equation (1) can be transformed into the formula for calculating the residual voltage value in the ferritic and austenitic phase as:

$\sigma_{fer} = 1{,}707*(N_{90} - N_0)$ (Mpa)

$\sigma_{aus} = 3{,}670*(N_{90} - N_0)$ (Mpa)

RESULTS AND DISCUSSION

Tensile Tests

Analyzing the results obtained, it is observed that all results were higher than the minimum required by the ASTM A240 standard for UNS S 31803 duplex steel, as shown in table 5.

Table 5 - Required Values x Values Obtained in the Traction Test

Specimen	Tensile Strength (MPa)*	Flow Limit (MPa)	Stretching (%)
SP1	757,46	561	32,15
SP2	709,75	547	31,07
SP3	765,76	572	33,72
Average	**744,32**	**560**	**32,31**

**required 620 MPa; **required 450 MPa; ***required 25%*

It was found that during the tensile test, the specimens broke in the base metal, indicating that the welding parameters were properly specified and applied. Thus, both the heat-affected zone and the weld metal have a higher mechanical strength than the base metal. The appearance of the fracture obtained in the tensile test is of the cup-cone type, typical of ductile materials (Figure 5).

Figure 5 - Some Types of Fractures - (a) "cup-cone" type; (b) Fragile; (c) Mixed; (d) Fragile; (e) Rosette; (f) Shear.

From the data collected in the tensile test, it was possible to trace the stress x strain graph of the three specimens tested, as shown in Figures 6 to 8, below. Analyzing this graph, it can be concluded that all specimens met the minimum required in terms of tensile strength (minimum of 620 Mpa) and deformation (minimum of 25%).

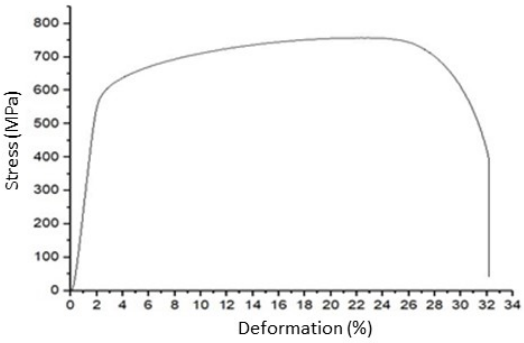

Figure 6 - Stress x Deformation SP 1 graph

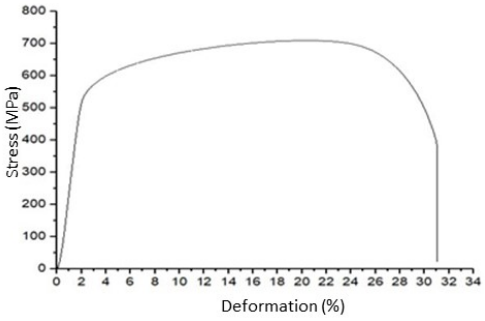

Figure 7 - Stress x Deformation SP 2 graph

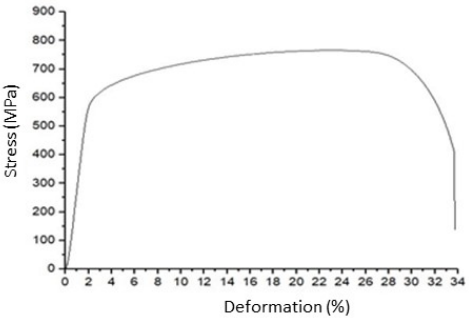

Figure 8 - Stress x Deformation SP 3 graph

Metallographic Analysis

The figures below show the microstructural characteristics of the duplex steel, observed by optical microscopy at 50X magnification, the base metal, thermally affected zone and weld metal were analyzed. Figure 9 demonstrates the analyzed specimen, after chemical attack with glyceregia.

Figure 9 - Specimen analyzed.

Micrography

In figure 10 it is possible to observe the microstructure of the base metal formed by two phases, in a mixture of about 50% by volume in islands of austenite (light gray) and 50% of ferrite grains (dark gray).

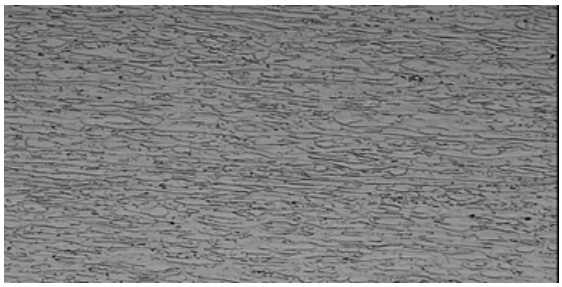

Figure 10 - 50x Optical Microscopy - Base metal

Figure 11 shows that the thermally affected zone, there were changes in the shape of the structure and with a slight increase in the percentage of ferrite.

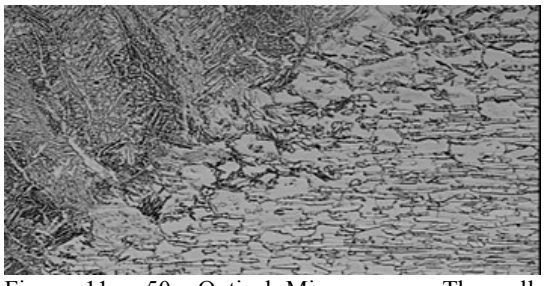

Figure 11 - 50x Optical Microscopy - Thermally Affected Zone (ZTA).

The metallographic analysis of the weld metal, represented in figure 12, shows the predominance of ferrite. This makes the weld metal a susceptible region to pitting corrosion in chloride-containing environments.

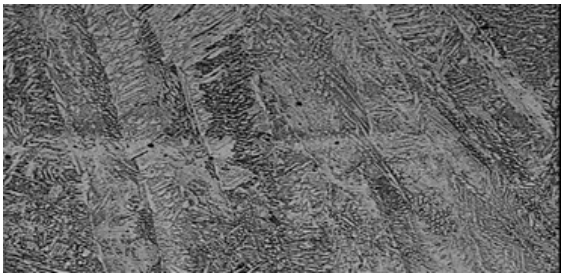

Figure 12 - 50x Optical Microscopy - Weld Metal

Residual Stress Analysis

Residual stress measurements were performed by x-ray diffraction in the weld bead, in the HAZ, HAZ+6 mm and at the weld root. Measurements were made in the ferritic and austenitic phases in the longitudinal and transverse directions in relation to the weld bead orientation.

The results showed tensile stresses in the weld bead, both in the longitudinal and transverse directions. In the HAZ, HAZ+6 and in the root, it showed compressive stresses in the transverse direction and tensile stresses in the longitudinal direction. The values of residual stresses by x-ray diffraction in the ferritic and austenitic phases of the duplex steel sheet are determined from graphs $\theta = f(\sin 2\psi)$ shown in figures 13 and 14.

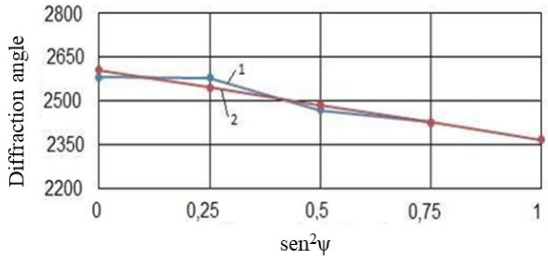

Figure 13 - Diffraction angle vs sin2ψ graph for measuring transverse stresses at the center of the weld bead for ferritic phase: *1 – experimental data; 2– line by linear regression.*

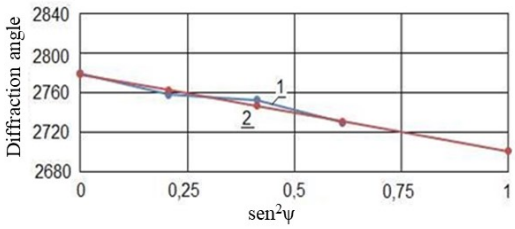

Figure 14 - Diffraction angle vs sin2ψ graph for measuring transverse stresses at the center of the weld bead for austenitic phase: *1 – experimental data; 2 – line by linear regression*.

Table 5 - Results of residual stress measurements on duplex steel sheet

Location	Ferrite		Austenite	
	Transverse tension	Longitudinal tension	Transverse tension	Longitudinal tension
Weld bead	395	285	280	150
ZTA	-220	150	-40	80
ZTA+ 6 mm	-110	100	-10	30
Root	-300	240	-100	180

CONCLUSIONS

In this paper, the impacts on the mechanical properties, on the metallographic behavior and the analysis of the residual stresses caused in an ASTM A240 UNS S31803 duplex stainless steel after the coated electrode welding process were analyzed and the main considerations in this regard were presented, data that the designer must consider when manufacturing equipment in duplex steel S31803.

The results for the tensile test of the present study were satisfactory, with the specimens breaking in the base metal. Indicating that the welding parameters used met the mechanical property requirements of the material.

The metallographic analysis showed an increase in the ferritic phase in the region of the weld bead, which makes this region preferable for pitting corrosion in chloride-containing media.

Residual stress measurements in duplex steel show tensile stresses in the weld bead in both directions (longitudinal and transverse). While in the ZTA, ZTA+6 mm and in the root presented compressive stresses in the transverse direction and tensile stresses in the longitudinal direction. The emergence of these stresses occurred during the cooling of the weld bead metal.

ACKNOWLEDGEMENTS

The authors would like to thank the financial support given by the Research Support Foundation of the State of Rio de Janeiro (FAPERJ) to the study.

REFERENCES

Alvarez-Armas, I. Duplex Stainless Steels: Brief history and some recent alloys, Recent Patents on Mechanical Engineering, vol. 1, pp. 51-57, 2008.

ASM HANDBOOK. Properties and Selection: Irons, steel and high performance alloys, ASM International, 1990.

Chang, P. H.; TENG, T. L. Numerical and experimental investigations on the residual stresses of

the butt-welded joints. Computational Material Science vol. 29, pp. 511-522, 2004.

Chen, T. H., YANG, J. R. Effects of solution treatment and continuous cooling on the σ-phase precipitation in a 2205 duplex stainless steel. Materials Science and Engineering A, vol. 311, pp. 28-41, 2001.

Evangelista, E., Mc QUEEN, H. J., NIEWCZAS, M., CABIBBO, M. Hot Workability of 2304 and 2205 Duplex Stainless Steels. Canadian Metallurgical Quarterly. vol. 43, 3, p. 339-354, 2004.

Folkhard, E. Welding Metallurgy of Stainless Steels. Springer-Verlag, Áustria, pp. 140-143, 1997

Gunn, R. N. Duplex stainless steels: microstructure, properties and applications. Cambridge, England: Abington Publishing. 204 p., 2003.

Karlsson, L; PAK, S. Welding of duplex stainless steels-properties of SMAW, FCAW and SAW welded joints. Conference Duplex Stainless Steel's91-Proceedings, Beaune, Bourcogne-França, p. 413-420, 1991.

Loureiro, J.P. Caracterização do aço inoxidável duplex UNS S31803 pela técnica não destrutiva de correntes parasitas pulsadas, Rio de Janeiro, UFRJ, Escola Politécnica, p. 97-102, 2010.

Marques, V. P., MODENESI, P.J., BRACARENSE, A.Q., SOLDAGEM – Fundamentos e Tecnologia, Editora UFMG, 2. Ed., 2007.

Monine, V.I., Teodosio, J. R., Ivanov, S. A., New methods of X ray tensometry. Advances in Experimental Mechanics, 1994.

Pinto, P. S. G. Avaliação da resistência ao impacto de juntas de aço inoxidável superduplex soldadas por GMAW pulsado com diferentes misturas gasosas. Tese de mestrado. Programa de Pós Graduação em Engenharia de Minas, Metalúrgica e de Materiais, PPGEM/UFRGS, 2009.

Ribeiro, A. A. F.; Ferreira, C. A. M.; SOUZA, M. C. L and TAPANES, N. C. O. Study of materials and welding used in the construction of racks for storage of fuel elements at nuclear plants. Engenharia Térmica (Thermal Engineering), vol. 20, 3, p. 31-36, 2021.

Sieurin, H. Fracture toughness properties of duplex stainless steels. Dissertação de doutorado, Royal Institute of Technology. Stockholm, Suécia. Maio, 2006.

Ueda, Y. Fukuda, K. Endo, S., "A study on the accuracy of estimated residual stresses by the existing measuring methods". In: Transactions of the Japan Welding Research Institute, 1975.